

# Robustness of intra-atomic frequency comb based quantum memory against fluctuating environment

G. P. Teja<sup>1</sup> and Sandeep K. Goyal<sup>1,\*</sup>

<sup>1</sup>*Indian Institute of Science Education and research,  
Mohali, Punjab 140306, India*

In this article, we study the robustness of the intra-atomic frequency comb (I-AFC) based quantum memory against various environmental factors. The effect of the environment is incorporated as random fluctuations in the parameters such as comb spacing and the optical depth, of the frequency comb. We also study the effect of temperature on the quality of the quantum memory which is quantified in terms of the efficiency of the photon storage. We found that the I-AFC is viable for photon storage even for very large fluctuations in the parameters of the frequency comb. Moreover, the temperature has a negligible effect on the quality of I-AFC. Our study conclusively establishes the tenacious nature of the I-AFC.

## I. INTRODUCTION

Quantum memory is a device which can store and reemit photons on demand. Quantum memory is essential for photonic quantum information processing and long-distance quantum communications [1–3]. Along with probabilistic single-photon sources, it can also be used to achieve deterministic single-photon sources [4, 5]. Among the atomic ensemble based quantum memories electromagnetically induced transparency [6–12], controlled reversible inhomogeneous broadening [13–18], gradient echo memory [19–22], Raman quantum memory [23–26] and the atomic frequency combs (AFCs) [27–33] are the most prevalent protocols for photonic quantum memory. The basic idea behind an atomic ensemble based quantum memory is the controlled reversible transfer of information between the light field and the atomic states. The incoming photons are made to interact with the ensemble of atoms and the excitation is transferred to a long-lived state. Reversing the process results in the photon emission.

Atomic frequency comb based quantum memory relies in artificially created frequency comb by reshaping the inhomogeneously broadened spectrum by means of optical hole burning in an ensemble of atoms. The incoming photon is absorbed as a delocalized excitation over the frequency comb. The comb-like structure of the atomic spectrum results in a photon-echo at a later time; hence the frequency comb serves as a delay line for the photon. To achieve a on-demand quantum memory, the excitation can be transferred to a long-lived spin state by applying an appropriate  $\pi$ -pulse. By applying another  $\pi$ -pulse the excitation can be transferred back to the excited state which will be emitted in the photon-echo.

In the AFC based quantum memory, the photons are stored as a delocalized excitation over all the teeth of the frequency comb which are consist of billions of atoms. Therefore, in order for AFC to work the entire atomic ensemble must behave like a single quantum

system. A small relative fluctuation in the frequencies of different atoms may give rise to strong decoherence in the frequency comb resulting in no photon-echo. This restricts the temperature range of AFC based quantum memory to a few Kelvins.

The intra-atomic frequency comb (I-AFC) based quantum memory is operationally similar to the one using AFC [33]. The difference being that the frequency comb in I-AFC is constructed using the degenerate hyperfine energy levels of an atom. The degeneracy in the hyperfine levels is lifted by applying external magnetic field. Since the frequency comb is realized with the atomic transition within each atoms, the perfect coherence between various teeth of the frequency comb is inherently ensured. This feature of I-AFC makes them robust against some of the temperature effects such as Doppler broadening [33]. Since, the frequency comb is built in individual atoms, the I-AFC is capable of providing quantum memory at the level of single atoms. However, there are certain limitations of I-AFC which may affect the efficiency of quantum memory.

One of the limitation of the I-AFC is that the frequency comb is not always uniform. The non-uniformity can be due to unequal absorption or due to unequal spacing between different hyperfine states. Non-uniformity of the frequency comb can cause low-efficiency for the storage of photons. Although the Doppler broadening due to temperature does not affect the I-AFC, the incoherent thermal distribution in the ground state manifold can result in lowering the efficiency. In this article, we numerically study the effect of all these adversities on the efficiency of the I-AFC based quantum memory. Effect of random fluctuations in the absorption and the comb spacing is incorporated by introducing randomness in the said parameters stochastically and then the average is taken over a number of trials. The effects of temperature on the I-AFC is studied by calculating the density matrix for the I-AFC system and calculating the photon-echo explicitly.

Our study shows that the fluctuations in different parameters in the I-AFC affect the efficiency of the photon storage differently. For example, the fluctuations

\* [skgoyal@iisermohali.ac.in](mailto:skgoyal@iisermohali.ac.in)

in the absorption in different teeth of the comb, i.e., non-uniformity in the height of the teeth has negligible effect on the efficiency. Whereas the fluctuations in the comb spacing has significant effect. Although, the effect of the comb spacing is stronger than the non-uniform absorption, we have high efficiency even for large fluctuations. Furthermore, this adverse effect can be easily mitigated by increasing the finesse of the frequency comb, which can be done by increasing the external magnetic field. We also see that the incoherent thermal population of the ground states of the I-AFC only affect the absorption of different transitions, Temperature has negligible effect on the efficiency. Hence, our study conclusively establish the tenacious nature of I-AFC as a quantum memory against a large class of environmental effects.

The article is organised as follows: in Sec. II we introduce the concepts useful to understand our results and calculations. Here we briefly explain the concept of AFC and I-AFC based quantum memory and the calculations for photon-echo efficiencies in the forward and backward propagation. In Sec. III we present our results and numerical simulations for the effect of random environment on the efficiency in I-AFC. We conclude in Sec. IV.

## II. BACKGROUND

In this section, we discuss the topics which are relevant for results presented in this article. We start by discussing the AFC protocol for quantum memory followed by I-AFC protocol.

### A. AFC

AFC typically consists of rare-earth ions doped in a dielectric crystal [27, 28, 30, 31, 34–36]. The rare-earth ions when doped in crystals experience in-homogeneously broadened spectral lines due to their interaction with the local environment in the host material. This spectrum can be reshaped by applying narrow-band lasers to transfer a fraction of population of ions corresponding to a chosen frequency to a stable auxiliary state, resulting in a hole in the spectrum. Repeating the process at desired frequencies reshapes the spectrum to yield a comb like structure [Fig. 1(a)]. In a uniform AFC, the spacing between the neighboring teeth of the comb is fixed (say  $\Delta$ ) and every tooth has a width of  $\gamma$ . In the approximation that  $\gamma \ll \Delta$  the frequency of the  $n$ -th tooth can be written as  $\delta_n = \omega_0 + n\Delta$  around some mean frequency  $\omega_0$ . The total size of the frequency comb is  $\Gamma = (2N + 1)\Delta \gg \Delta$  for  $2N + 1$  number of teeth.

When a photon of spectral width  $\gamma_p \gg \Delta$  is absorbed in the AFC with  $2N + 1$  number of teeth, the state of the

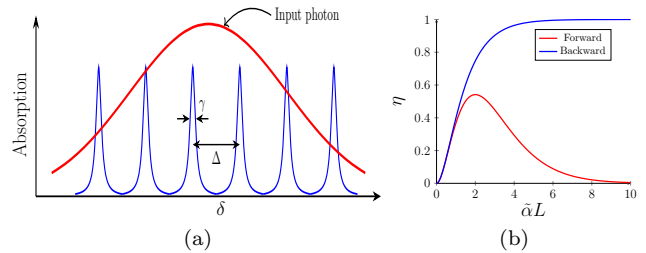


FIG. 1. (Color online) (a) AFC with tooth width  $\gamma$  and comb spacing  $\Delta$ . The red curve shows the spectrum of width  $\gamma_p$  of the incoming photon which interacts with the AFC. For the AFC to work efficiently  $\gamma_p \gg \Delta$ . (b) Forward and backward efficiency  $\eta$  for AFC as a function of optical depth  $\tilde{\alpha}L$ .

AFC can be formally written as [37, 38]

$$|\Psi\rangle_{\text{AFC}} = \sum_{j=1}^M \left( c_j e^{i\delta_j t} |\{e_j\}\rangle \prod_{k \neq j} |\{g_k\}\rangle \right). \quad (1)$$

Here  $|\{g_j\}\rangle$  and  $|\{e_j\}\rangle$  represent the ground and collective single-excitation state of all the atoms with detuning  $\delta_j$ , respectively, and the  $c_j$ 's represent the absorption coefficient of each tooth in the comb.

The probability of photon emission from the AFC is  $P(t) = |\sum_{j=-N}^N c_j e^{i\delta_j t} \rangle^2$  where we have used  $\delta_j = j\Delta$ . The  $P(t)$  vanishes at all times  $t$  except for  $t_n = 2n\pi/\Delta$  for positive integers  $n$  resulting in  $n$ -th photon-echo.

The collective dynamics of electric field and the atomic state of the AFC in the weak field approximation is governed by the following Maxwell-Bloch equations [8, 39]

$$\frac{\partial \sigma_{ge}}{\partial t} = -i\delta\sigma_{ge} + id_{eg}\mathcal{E}(z, t), \quad (2)$$

$$\frac{\partial}{\partial t} \pm c \frac{\partial}{\partial z} \mathcal{E}(z, t) = i \frac{\omega_L d_{ge}}{2\epsilon_0 V} \int n(\delta) \sigma_{ge}(z, t, \delta) d\delta. \quad (3)$$

Here  $n(\delta)$  is the atomic spectral distribution which characterize the AFC,  $\delta = \omega_L - \omega_{eg}$  is the detuning between light  $\omega_L$  and atomic transition  $\omega_{eg}$ . The  $\sigma_{ge} \equiv \sigma_{ge}(z, t)$  is the polarization operator in the Heisenberg picture,  $d_{eg}$  is the transition dipole matrix element for the transition  $|e\rangle - |g\rangle$ . The  $\pm$  sign in Eq. (3) represent the forward and backward propagating modes of light. For the case of forward propagating modes, solving these equations yields the output electric field  $\mathcal{E}_f$  as a function of  $z$  and the frequency  $\omega$ , which reads

$$\mathcal{E}_f(z, \omega) = \mathcal{E}_f(0, \omega) e^{-\mathcal{D}z}. \quad (4)$$

The input and the output electric field are related by the propagator  $\mathcal{D}$  which is given by

$$\mathcal{D} = -i\alpha \int \frac{n(\delta)}{\omega + \delta} d\delta - \frac{i\omega}{c}, \quad \alpha = \frac{|d_{eg}|^2 \omega_L}{2\epsilon_0 c V}. \quad (5)$$

Here  $\alpha$  is the absorption coefficient and  $V$  is the volume of the atomic ensemble.

In Principle, the electric field in the time domain  $\mathcal{E}_f(z, t)$  can be calculated by taking the inverse Fourier transform of  $\mathcal{E}_f(z, \omega)$ ; however, the expression for the same will be very cumbersome. In the limit  $\Gamma \gg \gamma_p \gg \Delta$ , and after propagating the electric field for a distance  $L$ , a simplified expression for  $\mathcal{E}_f(L, t)$  can be written as [28]

$$\mathcal{E}_f(L, t) = e^{-(\sqrt{2}\pi/\mathcal{F})^2} \left( \tilde{\alpha} L e^{-\tilde{\alpha} L/2} \right) \mathcal{E}_f(0, t - 2\pi/\Delta), \quad (6)$$

with  $\tilde{\alpha} = \alpha/\mathcal{F}$  and the finesse  $\mathcal{F}$  of AFC is the ratio between comb spacing and tooth width, i.e.,  $\mathcal{F} = \Delta/\gamma$ .

The AFC on its own results in a photon-echo which can be thought of as a delay line which is typically of the order of microseconds and solely depends on the comb spacing  $\Delta$ . In order to achieve on-demand retrieval of the input photon the excitation is transferred from the  $|e\rangle$  state to a long-lived spin state  $|s\rangle$  by applying a  $\pi$ -pulse. After the storage time (limited by the lifetime of the spin state  $|s\rangle$ ) a second  $\pi$ -pulse is applied to transfer the excitation back to  $|e\rangle$  which due to AFC will re-phase after time  $2\pi/\Delta$  [30]. Thus, one can achieve an on-demand and deterministic quantum memory.

Application of two  $\pi$ -pulses results in the overall sign change in the electric field which causes backward propagation of light. If we apply the  $\pi$ -pulses at time  $t = \pi/\Delta$  the atomic polarization induced by the input electric field will act as the source term for the backward field propagation. On solving the Maxwell-Bloch equations, the electric field in the backward mode can be written as [28]

$$\mathcal{E}_b(L, t) = e^{-(\sqrt{2}\pi/\mathcal{F})^2} (1 - e^{-\tilde{\alpha}L}) \mathcal{E}_f(0, t - 2\pi/\Delta), \quad (7)$$

which is same as forward mode solution apart from the factor  $1 - e^{-\tilde{\alpha}L}$  instead of  $\tilde{\alpha} L e^{-\tilde{\alpha}L/2}$ .

The quality of the quantum memory is quantified by the efficiency  $\eta$  which is defined as the ratio of the intensity of light in the first echo to the input light, i.e.,

$$\eta = \frac{\int_{\pi/\Delta}^{3\pi/\Delta} |\mathcal{E}(L, t)|^2 dt}{\int |\mathcal{E}(0, t)|^2 dt}. \quad (8)$$

For high finesse ( $\mathcal{F} \gg 1$ ) the efficiency for the forward propagating modes of light becomes  $\eta_f = (\tilde{\alpha}L)^2 \exp(-\tilde{\alpha}L)$  which can approach to a maximum value of 54% for  $\tilde{\alpha}L \equiv \alpha L/\mathcal{F} = 2$  (Fig. 1(b)). Since  $\mathcal{F} \gg 1$  the forward mode requires high absorption ( $\alpha L > \mathcal{F}$ ) for maximum efficiency. The efficiency in the backward mode is  $\eta_b(L) = (1 - e^{-\tilde{\alpha}L})^2$  which can be optimized over absorption and finesse to reach 100% (Fig. 1(b)).

Due to the strong interaction between the phonons in the crystal and the rare-earth ions, AFCs are typically realized at low temperatures ( $< 5\text{K}$ ), making it difficult for commercial use. Beyond these temperatures, the phase coherence between the different atoms in the

frequency comb is lost and the AFC does not work as a single quantum system. To overcome this problem one can exploit the degeneracy in the atomic states of alkali atoms to realize a frequency comb. Such frequency combs are called I-AFC, which is introduced in the following subsection.

## B. I-AFC

In I-AFC we start by considering an optical transition between hyper-fine degenerate energy levels  $\{|g_m\rangle\}$  and  $\{|e_n\rangle\}$  of an alkali atom. The degeneracy in the excited and ground states is lifted by applying external magnetic field with splitting proportional to magnetic field. Collectively, all the dipole allowed transitions between the ground state manifold and the excited state manifold yield a comb like structure similar to the one in Fig. 1(a), which is known as I-AFC [33].

The propagation of electromagnetic field through an ensemble of atom possessing I-AFC can be calculated using the Maxwell-Bloch equations. The propagator  $\mathcal{D}$  and absorption coefficient  $\alpha$  for the dynamics reads

$$\mathcal{D} = \sum_{nm} \frac{\alpha_{nm}}{1/2 + i/\gamma(n\Delta + \omega)} + \frac{i\omega}{c}, \quad (9a)$$

$$\alpha_{nm} = \mathcal{N} \rho_{mm} \frac{|d_{nm}|^2 \omega_L}{2\hbar\epsilon c\gamma}. \quad (9b)$$

This results in the output electric [33]

$$\mathcal{E}(L, \omega) = \mathcal{E}(0, \omega) e^{-\mathcal{D}L}, \quad (10)$$

where  $\mathcal{E}(0, \omega)$  is the input pulse with the mean frequency  $\omega_L$ . Here  $\gamma$ ,  $\mathcal{N}$  and  $d_{nm}$  are the tooth width, number density of atoms and the transition dipole moment between  $n$ th excited and  $m$ th ground state.

For simplicity we have assumed here that the spacing between the teeth of the comb  $\Delta$  is uniform. In real system such as Cesium atoms, the comb spacing (controlled by external magnetic field) and the absorption coefficient of each of the tooth can be non-uniform.

Similar to AFC, the dynamics of the electric field in I-AFC is completely characterized by the propagator  $\mathcal{D}$ , which in turn is controlled by the finesse  $\mathcal{F}$  and absorption coefficient  $\alpha$ . Despite the differences between the propagators of AFC and I-AFC [Eqs. (5) and (9a)], they yield similar results for photon-echo and efficiencies favoring high finesse and optical depths [33].

The calculations for the forward efficiency  $\eta_f$  in I-AFC can be done by calculating the ratio between the intensities in first echo and the total input intensity, as given in Eq. (8). However, the efficiency for the back scattering  $\eta_b$  requires an indirect approach [33]. In order to calculate  $\eta_b$ , first we estimate the average  $\tilde{\alpha}$  for I-AFC by comparing the I-AFC data with the AFC data for the forward propagation. By comparing forward

efficiencies of I-AFC with the Eq. (6) we obtain the common overall factor ( $e^{-(\sqrt{2}\pi/\mathcal{F})^2}$ ) which along with  $\tilde{\alpha}$  is used to calculate the backward efficiencies.

### III. RESULTS

Although, the propagation of light through I-AFC and AFC is identical, in physical scenario the efficiencies can be very different for the two. This is due to the fact that in AFC a uniform frequency comb can be constructed on demand and as desired; however, in I-AFC the shape of the comb is determined by the atomic structure. In general, naturally available frequency combs are not uniform. Moreover, the fluctuations in the applied magnetic field and spatial distribution of the atoms in the ensemble may also result in non-uniform frequency comb. There are several other factors which can cause low efficiency in I-AFC. In this section, we address the effects of (i) random comb spacing, (ii) random optical depth, and (iii) thermal effects on the efficiency in I-AFC.

Since each of the atom in the ensemble possesses its own frequency comb and the atoms are in an incoherent mixture, the light emitted from each atom contributes incoherently in the total outcome, i.e.,  $|\mathcal{E}_{\text{total}}|^2 = \sum_n |\mathcal{E}_n(z, t)|^2$ . Here  $\mathcal{E}_n$  is the light emitted by the  $n$ -th atom.

For the purpose of calculations, we consider an I-AFC with a total of seven teeth and light pulse with Gaussian spectrum of the following form:

$$\tilde{\mathcal{E}}(0, \omega) = \exp\left[-\frac{\omega^2}{2(2\Delta)^2}\right], \quad (11)$$

where  $\Delta$  is the comb spacing. The total spectral width of the photon is chosen in such a way that it covers all the seven peaks of the frequency comb.

#### A. Non-uniform comb spacing

We start with random spacing between the teeth of the comb as that is the most common trait in I-AFC. In order to introduce the randomness in the comb spacing, we randomly shift each of the tooth of an otherwise uniform comb. Hence,  $n$ -th tooth acquires a random shift  $\gamma_r^n$  which is a random number in some limit  $[-\gamma_r, \gamma_r]$ . In this scenario, the propagator  $\mathcal{D}$  reads

$$\mathcal{D} = \sum_{n=-3}^3 \frac{\gamma \alpha_n}{\gamma/2 + i(n\Delta + \gamma_r^n + \omega)} + \frac{i\omega}{c}. \quad (12)$$

Each of the atoms in the ensemble has a frequency comb attached characterized by a different propagator  $\mathcal{D}$  due to randomness. In our numerical calculations, we calculate the output electric field from each of these atoms and calculate the intensity of the output light by adding the intensities from each of the atoms. Using this we

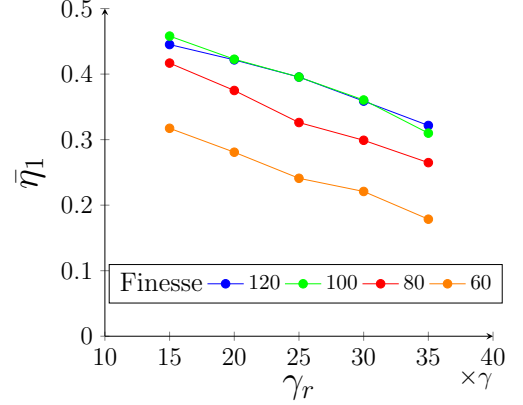


FIG. 2. (Color online) Here we have plotted the efficiencies as a function of the fluctuation strength  $\gamma_r$  of the comb spacing and for various values of the finesse  $\mathcal{F} = \Delta/\gamma$ . We have chosen the optical depth  $\beta = \alpha L = 30$  and tooth width  $\gamma = 5\text{MHz}$ . The fluctuation strength is measured in the units of the tooth width  $\gamma$ . From these plots we can see that although the efficiency is decreasing as we increase the randomness, the efficiencies are significant even at very large fluctuations.

calculate the forward and backward efficiency for this configuration and average it over a large number of trials.

In Fig. 2 we plot the forward efficiencies as a function of randomness  $\gamma_r$  for different values of finesse  $\mathcal{F}$ . Here  $\gamma_r$  is taken as a multiple of the tooth width  $\gamma$ . we observe that the efficiency drops with increasing randomness. However, increasing the finesse results in higher efficiency. In these plots, we have kept the finesse such that the neighboring teeth do not merge due to random fluctuations. One of the most striking conclusion we can draw from these plots is that the I-AFC is very robust against large fluctuations in the comb spacing.

In order to calculate the efficiency in the backward propagating modes, we need to compare the efficiency plots for the I-AFC and AFC as functions of the propagation length  $L$  and calculate the absorption coefficient  $\tilde{\alpha}$ , which will be used to estimate the efficiency in the backward mode. In Figs. 3(a)-3(d) we plot the forward efficiencies of AFC (solid curves) and I-AFC (dots) for various values of the finesse  $\mathcal{F}$ . We notice that for randomness  $\gamma_r > 25\gamma$  in Figs. 3(c) and 3(d) the two efficiencies do not match which makes the calculations of the backward efficiencies difficult. For randomness  $< 20\gamma$  Figs. 3(a)-3(b) we can see strong overlap between AFC and I-AFC. Using these plots we calculate the efficiency in the back scattering for randomness  $15\gamma$  and  $20\gamma$  which are close to 85% and 80%, respectively (Figs. 3(e)-3(f)). Interestingly, the efficiency in these plots shows improvement as we increase the finesse which can easily be achieved by increasing the external magnetic field. Therefore, the effect of the fluctuations in the comb spacing on the efficiency can easily be mitigated.

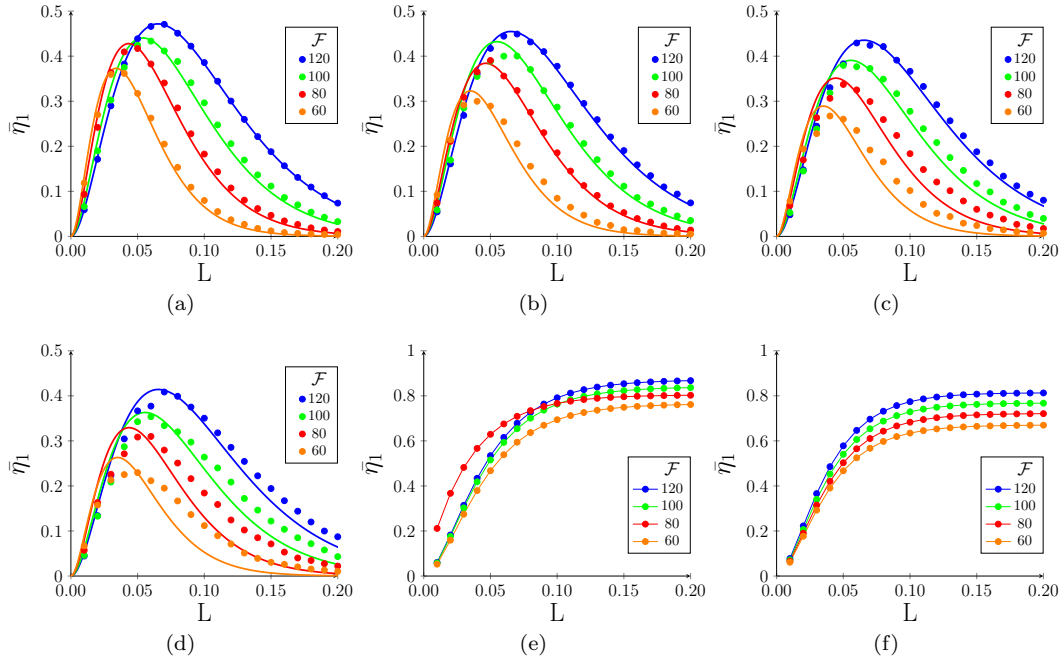


FIG. 3. Forward mode efficiencies vs length in I-AFC (dots) and AFC (lines) for the randomness  $15\gamma$  (a),  $20\gamma$  (b),  $25\gamma$  (c) and  $30\gamma$  (d). Backward mode efficiencies of I-AFC for the randomness  $15\gamma$  (e),  $20\gamma$  (f). In the inset are the different values of finesse

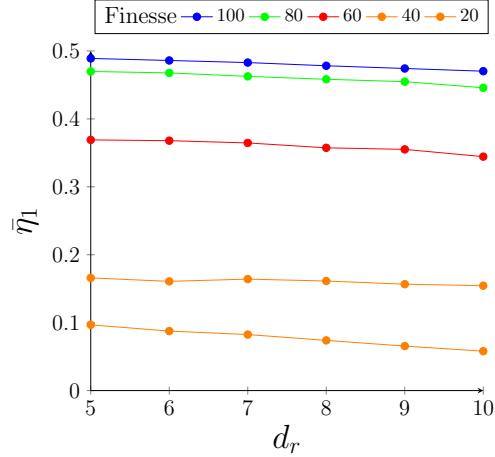


FIG. 4. Incoherent efficiencies as a function of fluctuation strength in optical depth  $\alpha L$ , respectively. Here the average optical depth  $\alpha L = 30$  and  $\gamma = 5\text{MHz}$ . Here we can see that the efficiencies increase with finesse and the strength of the fluctuation has negligible effect on the efficiencies.

### B. Non-uniform optical depths

The optical depth of various teeth in I-AFC in natural atoms is non-uniform in general. The non-equal transition probability between different atomic states is one of the biggest contributor to such non-uniformity. This can be further exaggerated by random environmental effects. Assuming the worst, in this

section we study the effect of fluctuation in the optical depths of different teeth of the I-AFC on the efficiency of the quantum memory. Similar to Sec. III A, we incorporate the fluctuating optical depth in I-AFC dynamics by adding randomness in the propagator  $\mathcal{D}$  as follows

$$\mathcal{D} = \sum_n \frac{(\alpha_n + d_r^n)}{1/2 + i/\gamma(n\Delta + \omega)} + \frac{i\omega}{c}. \quad (13)$$

where  $d_r^n \in [-d_r, d_r]$  determine the fluctuations in the optical depth.

In Fig. 4 we plot efficiency as a function of the randomness  $d_r$ . The different curves are for different finesse ranging from  $\mathcal{F} = 20$  to  $\mathcal{F} = 100$ . Interestingly, the fluctuations in the optical depth has little effect on the overall efficiency. Even for fluctuations as large as a third of the average optical depth the efficiency is almost the same. Therefore, we can conclude that the fluctuations in the optical depth does not play any major role in the photon-echo or the efficiency of the quantum memory.

### C. Thermal distribution

Typically, thermal effects are the most significant contributor towards decoherence in any quantum system. This is considered to be the main cause of inefficient quantum memories at high temperatures. The thermal effects mainly reflect as Doppler broadening of the

transition lines in an atomic ensemble and as incoherent thermal distribution of the population of energy eigenstates. Since the frequency comb is attached with each of the atom in an I-AFC, the Doppler broadening has very little effect on the efficiency [33]. In this section we study the effect of thermal population distribution of the atomic energy levels on the efficiency in I-AFC.

The typical frequency of an optical transition ( $\sim 10^{15}$ Hz) is much greater than the thermal frequency ( $\sim 10^{13}$ Hz) at 100k; therefore, most of the atoms are found in the ground states. However, in an I-AFC the frequency comb is constructed using the transitions between the degenerate ground states and excited states. The degeneracy in the ground and excited states are lifted by applying external magnetic field which results in a frequency comb of ground states spanning few hundred Giga Hertz. At non-zero temperature the initial state of the atomic ensemble will be a thermal distribution over the ground states. Surprisingly in I-AFC, the only role of the ground state population  $\rho_{mm}$  is to affect the optical depth as shown in Eq. (9b). At temperature  $T$ , the population of the  $m$ -th ground state is given by  $\rho_{mm} = \exp(-E_m/K_bT)/Z$  where  $E_m$  is the energy of the  $m$ -th state,  $K_b$  is the Boltzmann coefficient and  $Z = \sum_m \exp(-E_m/K_bT)$  is the partition function. This will affect the absorption coefficient as [Eq. (9b)]:

$$\alpha_{nm} = \mathcal{N} \frac{|d_{nm}|^2 \omega_L \exp(-E_m/K_bT)}{2\hbar\epsilon\gamma} \frac{1}{Z}. \quad (14)$$

As we know from Sec. III B that the fluctuation in the optical depth has very little effect on the efficiency; we conclude that the I-AFC is robust against thermal effects.

#### IV. CONCLUSION

In conclusion, we have shown that the I-AFC based quantum memory is robust against a large class of

adversities. Since, I-AFC is realized in each individual atom of an ensemble, the non-uniformity in terms of the comb spacing and the teeth height is the biggest factor that can affect the quality of the quantum memory. On the other hand, temperature can cause decoherence in the frequency comb, destroying the capability to store and retrieve photons on demand. We numerically study the effect of all these non-uniformities and thermal environment on the quality of the I-AFC.

Various types of non-uniformities were incorporated by introducing random fluctuations in the concerned parameters and the efficiency of the photon-echo was calculated by averaging over many runs of the simulations. In our calculations, we found that the quality of the I-AFC persists even for large fluctuations in the comb spacing. Whatever little effect the fluctuations have on the efficiency of the quantum memory can be mitigated by increasing the finesse of the I-AFC by means of external magnetic field. Furthermore, the fluctuations in the teeth heights and the thermal environment has negligible effect on the quality of quantum memory. This conclusively establish the tenacious nature of the I-AFC and makes it one of the strongest candidates for high-temperature quantum memory.

#### ACKNOWLEDGMENTS

We acknowledge the financial support from Interdisciplinary Cyber Physical Systems(ICPS) programme of the Department of Science and Technology, India, (Grant No.:DST/ICPS/QuST/Theme-1/2019/12)

---

[1] L.-M. Duan, M. Lukin, J. I. Cirac, and P. Zoller, *Nature* **414**, 413 (2001).

[2] N. Sangouard, C. Simon, H. De Riedmatten, and N. Gisin, *Reviews of Modern Physics* **83**, 33 (2011).

[3] F.-Y. Zhang, X.-Y. Chen, C. Li, and H.-S. Song, *Scientific reports* **5**, 17025 (2015).

[4] S. Chen, Y.-A. Chen, T. Strassel, Z.-S. Yuan, B. Zhao, J. Schmiedmayer, and J.-W. Pan, *Physical review letters* **97**, 173004 (2006).

[5] H. Barros, A. Stute, T. Northup, C. Russo, P. Schmidt, and R. Blatt, *New Journal of Physics* **11**, 103004 (2009).

[6] M. Fleischhauer and M. D. Lukin, *Physical Review A* **65**, 022314 (2002).

[7] B. Julsgaard, J. Sherson, J. I. Cirac, J. Fiurášek, and E. S. Polzik, *Nature* **432**, 482 (2004).

[8] A. V. Gorshkov, A. André, M. D. Lukin, and A. S. Sørensen, *Physical Review A* **76**, 033805 (2007).

[9] Y.-W. Cho and Y.-H. Kim, *Phys. Rev. A* **82**, 033830 (2010).

[10] D. Höckel and O. Benson, *Phys. Rev. Lett.* **105**, 153605 (2010).

[11] Y. Wang, J. Li, S. Zhang, K. Su, Y. Zhou, K. Liao, S. Du, H. Yan, and S.-L. Zhu, *Nature Photonics* **13**, 346 (2019).

[12] N. Jiang, Y.-F. Pu, W. Chang, C. Li, S. Zhang, and L.-M. Duan, *npj Quantum Information* **5**, 1 (2019).

[13] M. Nilsson and S. Kröll, *Optics Communications* **247**, 393 (2005).

[14] A. L. Alexander, J. J. Longdell, M. J. Sellars, and N. B. Manson, *Physical Review Letters* **96**, 1 (2006), 0506232.

[15] B. Kraus, W. Tittel, N. Gisin, M. Nilsson, S. Kröll, and J. I. Cirac, *Physical Review A - Atomic, Molecular, and Optical Physics* **73**, 1 (2006), 0502184.

[16] N. Sangouard, C. Simon, M. Afzelius, and N. Gisin, *Physical Review A - Atomic, Molecular, and Optical Physics* **73**, 1 (2006), 0502184.

Physics **75**, 1 (2007), 0611165.

[17] J. J. Longdell, G. Hétet, P. K. Lam, and M. J. Sellars, Physical Review A - Atomic, Molecular, and Optical Physics **78**, 1 (2008).

[18] I. Īakoupor and A. S. Sørensen, New Journal of Physics **15**, 085012 (2013).

[19] G. Hetet, J. Longdell, A. Alexander, P. K. Lam, and M. Sellars, Physical review letters **100**, 023601 (2008).

[20] B. M. Sparkes, M. Hosseini, G. Hétet, P. K. Lam, and B. C. Buchler, Phys. Rev. A **82**, 043847 (2010).

[21] M. Hosseini, B. M. Sparkes, G. Campbell, P. K. Lam, and B. C. Buchler, Nature communications **2**, 174 (2011).

[22] M. Hosseini, B. Sparkes, G. Campbell, P. K. Lam, and B. Buchler, Journal of Physics B: Atomic, Molecular and Optical Physics **45**, 124004 (2012).

[23] K. F. Reim, J. Nunn, V. O. Lorenz, B. J. Sussman, K. C. Lee, N. K. Langford, D. Jaksch, and I. A. Walmsley, Nature Photonics **4**, 218 (2010).

[24] S. E. Thomas, J. H. Munns, K. T. Kaczmarek, C. Qiu, B. Brecht, A. Feizpour, P. M. Ledingham, I. A. Walmsley, J. Nunn, and D. J. Saunders, New Journal of Physics **19**, 063034 (2017).

[25] J. Guo, X. Feng, P. Yang, Z. Yu, L. Chen, C.-H. Yuan, and W. Zhang, Nature communications **10**, 148 (2019).

[26] A. Kalachev, A. Berezhnoi, P. Hemmer, and O. Kocharovskaya, Laser Physics **29**, 104001 (2019).

[27] H. De Riedmatten, M. Afzelius, M. U. Staudt, C. Simon, and N. Gisin, Nature **456**, 773 (2008).

[28] M. Afzelius, C. Simon, H. De Riedmatten, and N. Gisin, Physical Review A **79**, 052329 (2009).

[29] A. I. Lvovsky, B. C. Sanders, and W. Tittel, Nature photonics **3**, 706 (2009).

[30] M. Afzelius, I. Usmani, A. Amari, B. Lauritzen, A. Walther, C. Simon, N. Sangouard, J. Miná, H. De Riedmatten, N. Gisin, and S. Kröll, Physical Review Letters **104**, 1 (2010).

[31] M. Bonarota, J. Le Gouët, and T. Chaneliere, New Journal of Physics **13**, 013013 (2011).

[32] P. Jobez, N. Timoney, C. Laplane, J. Etesse, A. Ferrier, P. Goldner, N. Gisin, and M. Afzelius, Phys. Rev. A **93**, 032327 (2016).

[33] G. P. Teja, C. Simon, and S. K. Goyal, Physical Review A **99**, 052314 (2019).

[34] B. Lauritzen, J. Miná, H. De Riedmatten, M. Afzelius, and N. Gisin, Physical Review A **83**, 012318 (2011).

[35] N. Timoney, B. Lauritzen, I. Usmani, M. Afzelius, and N. Gisin, Journal of Physics B: Atomic, Molecular and Optical Physics **45**, 124001 (2012).

[36] Z.-Q. Zhou, J. Wang, C.-F. Li, and G.-C. Guo, Scientific reports **3**, 2754 (2013).

[37] R. H. Dicke, Physical review **93**, 99 (1954).

[38] M. Gross and S. Haroche, Physics reports **93**, 301 (1982).

[39] N. Sangouard, C. Simon, M. Afzelius, and N. Gisin, Physical Review A **75**, 032327 (2007).